ELSEVIER

Hydrothermal synthesis and structures of the open-framework copper silicates $Na_2[Cu_2Si_4O_{11}](H_2O)_2$ (CuSH-2Na), $Na_2[CuSi_3O_8]$ (CuSH-3Na), $Cs_2Na_4[Cu_2Si_{12}O_{27}(OH)_2](OH)_2$ (CuSH-4NaCs), and $Na_2[Cu_2Si_5O_{13}](H_2O)_3$ (CuSH-6Na)

Xiqu Wang [*], Lumei Liu, Lingbao Wang, Allan J. Jacobson

Department of Chemistry and Center for Materials Chemistry, University of Houston, Houston, TX 77204-5003, USA

Abstract

A series of open-framework copper silicates has been synthesized under mild hydrothermal conditions. The frameworks are based on double chains, single layers or double layers of SiO_4 tetrahedra interconnected by CuO_4 squares or tetrahedra or CuO_5 tetragonal pyramids. The structures contain 8-ring or 10-ring channel systems with apertures up to 2.7×5.9 Å which are filled by alkali metal cations and water molecules.
© 2005 Elsevier SAS. All rights reserved.

1. Introduction

Nanoporous crystalline materials with lattices of pores in the nanometer scale are of interest for applications in catalysis, gas separations and as ion-exchangers [1]. The best-known examples of nanoporous silicates are the zeolites which have open frameworks formed by interconnecting SiO_4 and AlO_4 tetrahedra [2]. The substitution of the aluminum and silicon by other metal cations including transition metals, in order to obtain porous frameworks with new properties has been studied in some detail. The framework topology is usually unchanged for substitutions at comparatively low levels [3]. On the other hand, substitutions at stoichiometric levels, particularly by non-tetrahedral cations often lead to new framework topologies [4]. Representative examples of such porous transition metal silicates include the titanium silicates ETS-4 and ETS-10 discovered in the late nineteen eighties [5] and a family of vanadium silicates reported more recently by our group and by others [6–10]. The framework transition metal sites provide additional ways to manipulate the redox and acid-base properties of these materials.

Several natural and synthetic copper silicates are known including cuprorivaite $CuCuSi_4O_{10}$ ('Egyptian Blue') and the recently reported mineral ajoite $(K,Na)_3Cu_{20}Al_3Si_{29}O_{76}(OH)_{16} \cdot 8H_2O$, found in Arizona porphyry copper hydrothermal deposits [11–13]. These and similar compounds suggest the feasibility of synthesizing porous copper silicate frameworks similar to the vanadium silicates; divalent copper ions, like vanadium (IV) and (V) ions, can form variously distorted coordination polyhedra with coordination numbers 4, 5 or 6 with oxygen anions leading to a range of possible framework types [14,15]. Using hydrothermal techniques under conditions comparable to those used in classical zeolite synthesis, we have obtained a series of nanoporous copper silicates that are designated as CuSH-nA where n is a framework type number and A represents the extra-framework cations. The CuSH-1, CuSH-2 and CuSH-3 phases were first described by us in 2002 [16,17]. Detailed data for the CuSH-1A ($A =$ Na, K, Rb and Cs) phases which have channel systems with an aperture 0.7×0.4 nm were reported subsequently [18]. Recently, Rocha and coworkers published the synthesis and structure of a copper silicate designated as AV-23 that appears to be identical to CuSH-2Na [19]. Here we report the synthesis and structural details of the open-framework copper silicates $Na_2[Cu_2Si_4O_{11}](H_2O)_2$ (CuSH-2Na), $Na_2[CuSi_3O_8]$

* Corresponding author. Fax: +1 713 743 2787; Tel.: +1 713 743 2780.
  E-mail address: xiqu.wang@mail.uh.edu (X. Wang).

(CuSH-3Na), $Cs_2Na_4[Cu_2Si_{12}O_{27}(OH)_2](OH)_2$ (CuSH-4NaCs), and $Na_2[Cu_2Si_5O_{13}](H_2O)_3$ (CuSH-6Na).

2. Experimental

2.1. Synthesis

The chemicals used for the syntheses were commercial reagent grade and were all used as purchased. The syntheses of the CuSH-nA compounds were carried out in Teflon-lined autoclaves under hydrothermal conditions at $240\,°C$. After an appropriate reaction time the autoclaves were removed from the oven and cooled down to room temperature in air. The products were vacuum-filtered, washed with water and dried in air at room temperature.

2.1.1. Syntheses of CuSH-2Na and CuSH-3Na

Blue needles of CuSH-2Na and dark blue plates of CuSH-3Na were first obtained in single crystal forms as minor impurities during the synthesis of CuSH-1Na. In order to investigate the phase field of each compound, a systematic synthesis study in the SiO_2–$Cu(OH)_2$–$NaOH$–H_2O system was performed in the presence of H_2O_2. $Cu(OH)_2$ was freshly precipitated by adding aqueous NH_4OH to a $Cu(NO_3)_2$ solution followed by thorough washing with deionized water and drying in air at $110\,°C$. In a typical experiment, $Cu(OH)_2$ was mixed with fumed silica and aqueous NaOH with appropriate ratios. The mixture was sealed together with H_2O_2 in a flexible Teflon bag in air. The bag was subsequently sealed in an autoclave filled with water to about 60% and heated at $240\,°C$ for 2d. In each experiment, the total number of moles of $Cu(OH)_2$, SiO_2 and NaOH were held at 0.01 mole and the water and H_2O_2 amounts were 1.5 ml and 0.3 ml respectively.

2.1.2. Synthesis of CuSH-4NaCs

For the synthesis of CuSH-4NaCs, solutions *A* and *B* were separately prepared by dissolving fumed silica (5.7 g) in aqueous CsOH (4.2 M, 18.8 ml) and aqueous NaOH (4.2 M, 27.0 ml), respectively. 0.26 ml of solution A and 1.08 ml of solution B were mixed with 363 mg $CuSO_4·5H_2O$. The mixture was sealed together with 0.6 ml H_2O and 0.1 ml H_2O_2 in a flexible Teflon bag in air. The bag was subsequently sealed in an autoclave filled with water to about 60% and heated at $240\,°C$ for 3 d.

2.1.3. Synthesis of CuSH-6Na

For the synthesis of CuSH-6Na, 0.9 g silica gel (Sigma S-4883) was mixed with 0.6 g NaOH, 0.1 g Cu and 0.04 g Ti metal foil. The mixture was placed in a Teflon tube with an open end. The tube was subsequently placed in a sealed Parr autoclave. The autoclave was filled with water to ${\sim}30\%$ inner volume and the water was kept outside the Teflon tube. After sealing in air, the autoclave was heated at $245\,°C$ for 4 d and then cooled to room temperature in air within 4 h.

2.2. Characterization

The compounds were analyzed by EDX using a JEOL JSM 6400 scanning electron microscope with a Link Analytical EXL spectrometer. Chemical analysis was made at Galbraith Laboratories, Knoxville, TN. Thermogravimetric analysis (TGA) was carried out on a DuPont 2100 TGA system. Infrared spectra were collected with a Galaxy FTIR 5000 series spectrometer using the KBr pellet method. Powder X-ray data were measured on a Sintag-XDS2000 diffractometer.

2.3. X-ray crystallography

Single crystal X-ray data were measured on a SMART platform diffractometer equipped with a 1K CCD area detector using graphite-monochromatized MoK_α radiation at 293 K. For each phase a hemisphere of data (1271 frames at 5 cm detector distance) was collected using a narrow-frame method with scan widths of $0.30°$ in ω and an exposure time of 30–80 s/frame. The data were integrated using the Siemens SAINT program [20]. Absorption corrections were made using the program SADABS [21]. The structures were solved by direct methods and refined using SHELXTL [22]. The crystallographic data are listed in Table 1. Atom positions are given in Table 2.

3. Results and discussion

3.1. Synthesis

The phase appearance fields in the SiO_2–$Cu(OH)_2$–$NaOH$–H_2O system are shown schematically in Fig. 1. In addition to the CuSH-nNa, $n = 1$–3, phases, polycrystalline CuO and unidentified amorphous phases were also found in the products. Both CuSH-2Na and CuSH-3Na were obtained as a major phase on the $Cu(OH)_2$-poor end of the corresponding phase field. Although optimal conditions for single-phase products have not yet been found for either phase, good quality single crystals suitable for detailed structural studies were readily obtained.
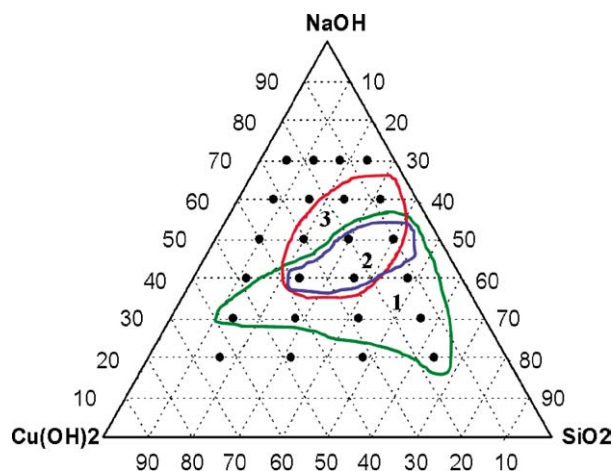

Fig. 1. Schematic plot of the phase fields in the SiO_2–$Cu(OH)_2$–$NaOH$–H_2O system. The dots represent the experiments performed. 1: CuSH-1Na, 2: CuSH-2Na, 3: CuSH-3Na.

Table 1
Crystal data and structure refinement details

	CuSH-2Na	CuSH-3Na	CuSH-4CsNa	CuSH-6Na
Formula	$H_4Cu_2Na_2O_{13}Si_4$	$CuNa_2O_8Si_3$	$H_4Cs_2Cu_2Na_4O_{31}Si_{12}$	$H_6Cu_2Na_2O_{16}Si_5$
F.W.	497.45	321.79	1321.97	575.56
Temperature/K	293(2)	293(2)	293(2)	243(2)
Space group	P-1	$P2_1/c$	$C2/c$	$P2/n$
a/Å	5.2254(7)	7.9324(5)	24.884(3)	11.161(1)
b/Å	6.4126(8)	10.3285(6)	7.261(1)	5.2135(6)
c/Å	8.516(1)	9.6005(6)	18.182(3)	11.813(1)
α/°	101.1(1)	90	90	90
β/°	94.3(1)	105.6(1)	113.2(1)	95.3(1)
γ/°	102.5(1)	90	90	90
V/Å^3	271.37(6)	757.55(8)	3020.0(7)	684.4(1)
Refl. collected/unique	1706/1193	4583/1726	9292/3509	4141/1600
R_{int}	0.0154	0.0315	0.0454	0.0164
Data/parameters	1193/106	1726/128	3509/238	1600/132
Goodness-of-fit	0.977	1.073	1.010	0.996
$R1/wR2$ $(I > 2\sigma(I))$	0.0334/0.0748	0.0292/0.0837	0.0403/0.0664	0.0247/0.0619
$R1/wR2$ (all data)	0.0574/0.0817	0.0333/0.0857	0.0751/0.0749	0.0320/0.0649

$R1 = \sum ||F_o| - |F_c||/\sum |F_o|$, $wR2 = [\sum(w(F_o^2 - F_c^2)^2)/\sum(wF_o^2)^2]^{1/2}$.

Pale purple needles of CuSH-4CsNa were obtained as a minor phase together with CuSH-1Cs and CuO. Green needles of CuSH-6Na were obtained as a minor phase together with Cu-ETS-4 [23] and unreacted Ti metal. For both CuSH-4CsNa and CuSH-6Na, extensive efforts to improve the yield by changing reagent ratios and reaction temperatures were made but have not yet succeeded.

3.2. Characterization

The chemical compositions measured by chemical analysis for CuSH-2Na and CuSH-3Na and atomic ratios measured by EDX analysis for CuSH-4CsNa and CuSH-6Na are consistent with the title formulae derived from crystal structure refinements. Calculated (%) for CuSH-2Na ($Na_2[Cu_2Si_4O_{11}]$-$(H_2O)_2$): Na 9.24, Cu 25.55, Si 22.59; found: Na 9.07, Cu 23.21, Si 23.10. Calculated (%) for CuSH-3Na ($Na_2CuSi_3O_8$): Na 14.29, Cu 19.75, Si 26.19; found: Na 14.17, Cu 18.25, Si 27.71. Observed atomic ratios for CuSH-4NaCs ($Cs_2Na_4[Cu_2$-$Si_{12}O_{27}(OH)_2](OH)_2$): Cu : Cs : Na : Si = 1 : 1.13 : 2.16 : 5.98, and for CuSH-6Na ($Na_2[Cu_2Si_5O_{13}](H_2O)_3$): Cu : Si = 1 : 2.24. During EDX analysis of the crystals of CuSH-6Na peaks for Na were observed but were quickly diminished in intensity probably owing to the instability of the crystals under the measurement conditions.

TGA for CuSH-2Na in air shows a weight loss of 7.12% below 390 °C, in good agreement with the theoretical value of 7.24% for the full dehydration. Powder X-ray diffraction patterns measured before and after TGA were closely similar, indicating the framework was largely intact upon dehydration. Similar dehydration behavior was reported for AV-23 [19].

Fig. 2 shows the IR data for CuSH-2Na and CuSH-4CsNa. The spectra have the expected features for polymerized silicate tetrahedra and intracrystalline water. The strong peaks due to the asymmetric stretching of the SiO$_4$ tetrahedra are observed in the frequency range of 900–1150 cm^{-1} for CuSH-2Na and 940–1160 cm^{-1} for CuSH-4CsNa. The peaks in the fre-
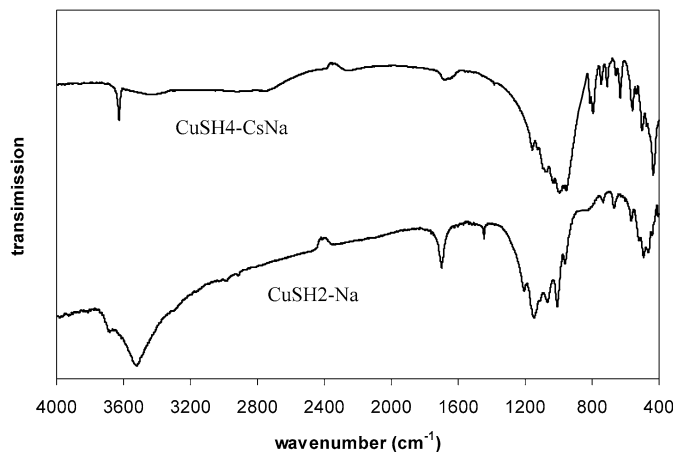

Fig. 2. The IR spectra for CuSH-2Na and CuSH-4CsNa.

quency range of 400–800 cm^{-1} are due to the Si–O–Si bending modes and internal symmetric stretching of the SiO$_4$ tetrahedra, which are substantially different for the two phases because of the different structures of the silicate anions. A sharp peak at 3627 cm^{-1} for the terminal Si–OH groups is observed for CuSH-4CsNa.

3.3. Crystal structure description

3.3.1. CuSH-2Na

The structure of CuSH-2Na contains double chains of SiO$_4$ tetrahedra that are interlinked by CuO$_5$ tetragonal pyramids to form a 3D framework (Fig. 3). The 3D framework is traversed by a 1D system of eight ring channels that are filled by sodium ions and water molecules. The silicate double chain has a periodicity of two tetrahedra and has intrachain six-rings. The CuO$_5$ pyramid has four Cu–O bonds with lengths 1.926(3)–1.977(3) Å in the base and a long apical Cu–O bond of 2.506(3) Å. The pyramids are interconnected by sharing common edges to form an infinite chain paral-

Table 2
Atomic coordinates ($\times 10^4$) and equivalent isotropic displacement parameters ($\text{Å}^2 \times 10^3$)

	x	y	z	U_{eq}
CuSH-2Na				
Na(1)	3614(3)	3640(3)	2024(2)	16(1)
Cu(1)	−2044(1)	1128(1)	683(1)	9(1)
Si(1)	5370(2)	1199(2)	−3119(1)	8(1)
Si(2)	1170(2)	3376(2)	−1686(1)	7(1)
O(1)	1088(6)	1725(5)	−454(3)	9(1)
O(2)	−4970(6)	420(5)	1915(4)	13(1)
O(3)	5000	0	5000	16(1)
O(4)	2307(6)	−4120(5)	−916(4)	12(1)
O(5)	−3213(6)	−2720(5)	3009(3)	10(1)
O(6)	8264(6)	2903(5)	−2753(4)	11(1)
O(7W)	760(8)	2688(7)	3890(4)	32(1)
H(1)	1290(100)	2310(90)	4710(40)	32(17)
H(2)	−540(90)	3200(110)	4060(70)	80(30)
CuSH-3Na				
Na(1)	−1998(2)	−249(1)	390(1)	22(1)
Na(2)	2073(2)	4898(1)	1293(1)	18(1)
Cu(1)	144(1)	2282(1)	1867(1)	10(1)
Si(1)	−3839(1)	−2833(1)	1081(1)	8(1)
Si(2)	−3814(1)	2288(1)	1935(1)	9(1)
Si(3)	1963(1)	−228(1)	3088(1)	9(1)
O(1)	−3462(2)	3825(2)	2257(2)	14(1)
O(2)	−722(2)	3962(2)	1165(2)	12(1)
O(3)	2393(2)	3071(2)	2902(2)	13(1)
O(4)	−2099(2)	1496(2)	1910(2)	13(1)
O(5)	1034(2)	563(2)	1637(2)	12(1)
O(6)	−5416(3)	−3279(2)	1774(2)	12(1)
O(7)	−2981(2)	−4173(2)	674(2)	11(1)
O(8)	−4656(3)	−2060(2)	−428(2)	14(1)
CuSH-4CsNa				
Cs(1)	222(1)	7662(1)	1186(1)	30(1)
Na(1)	2467(1)	2421(3)	1464(1)	22(1)
Na(2)	2823(1)	7515(3)	1709(1)	21(1)
Cu(1)	2389(1)	4885(1)	−133(1)	11(1)
Si(1)	1205(1)	4990(2)	76(1)	11(1)
Si(2)	1393(1)	9201(2)	301(1)	10(1)
Si(3)	−1336(1)	9693(2)	1286(1)	10(1)
Si(4)	595(1)	12487(2)	2424(1)	9(1)
Si(5)	1137(1)	5636(2)	3470(1)	10(1)
Si(6)	1090(1)	12347(2)	1222(1)	11(1)
O(1)	551(1)	12102(4)	1528(2)	11(1)
O(2)	−1068(1)	10085(5)	615(2)	16(1)
O(3)	1174(2)	7104(5)	359(2)	16(1)
O(4)	0	11828(7)	2500	14(1)
O(5)	−840(1)	5114(5)	898(2)	14(1)
O(6)	1110(2)	10334(5)	835(2)	17(1)
O(7)	1021(2)	7826(5)	3251(2)	14(1)
O(8)	720(1)	4649(4)	2627(2)	11(1)
O(9)	831(1)	3808(5)	477(2)	13(1)
O(10)	−1122(1)	11307(5)	1957(2)	15(1)
O(11)	2081(1)	9361(5)	626(2)	18(1)
O(12)	1805(1)	5057(5)	3777(2)	14(1)
O(13)	−2027(1)	9659(5)	943(2)	14(1)
O(14)	1842(2)	4189(5)	320(2)	16(1)
O(15)	1682(2)	2964(5)	1898(2)	17(1)
O(16)	2980(2)	1466(6)	2849(2)	32(1)
H(1)	1780(20)	4030(40)	2070(30)	26[b]
H(2)	3305(15)	1600(100)	3190(30)	48[b]

(continued)

Table 2 (*Continued*)

	x	y	z	U_{eq}
CuSH-6Na				
Na(1)	7351(1)	−2771(2)	5643(1)	18(1)
Cu(1)	5736(1)	2424(1)	5195(1)	8(1)
Si(1)	6163(1)	−4542(1)	2896(1)	6(1)
Si(2)	5201(1)	−558(1)	7330(1)	6(1)
Si(3)	7500	−8027(2)	7500	7(1)
O(1)	6081(2)	5294(4)	4228(2)	10(1)
O(2)	4653(2)	748(3)	4006(2)	8(1)
O(3)	7500	−4868(5)	2500	13(1)
O(4)	6834(2)	3556(4)	6471(2)	10(1)
O(5)	355(2)	−3205(4)	7205(2)	8(1)
O(6)	8482(2)	−57(4)	6990(2)	9(1)
O(7)	5689(2)	−1773(4)	2365(2)	9(1)
O(8W)	7825(2)	328(5)	4372(2)	30(1)
O(9W)[a]	9194(4)	−5124(11)	5098(4)	28(1)
H(1)	8180(30)	−130(80)	3810(20)	45[b]
H(2)	8230(30)	1540(60)	4680(30)	45[b]
H(3)[a]	9550(50)	−5140(170)	5750(20)	41[b]
H(4)[a]	9720(40)	−5340(190)	4650(40)	41[b]

U_{eq} is defined as one third of the trace of the orthogonalized U_{ij} tensor.
[a] Half occupied.
[b] Fixed at 1.5 times of the U_{eq} of the parent oxygen atoms.

lel to the silicate double chains. The pyramidal coordination of the Cu atom is complemented by a water oxygen atom at 2.884(3) Å to form a highly distorted $CuO_5(OH_2)$ octahedron. The sodium ion is bonded to four framework oxygen atoms at 2.327(4)–2.379(4) Å and two water oxygen atoms at 2.503(3)–2.601(4) Å. Hydrogen bonds occur between the water molecules and the framework oxygen atoms with an O···O distance 2.841(5) Å.

3.3.2. CuSH-3Na

The 3D framework of *CuSH-3Na* consists of single layers of SiO_4 tetrahedra cross-linked by distorted CuO_4 tetrahedra. The $CuSi_3O_8$ tetrahedral framework contains channel systems along the [100] and [010] directions which are filled by the extra-framework Na ions (Fig. 4). The silicate single layer is formed by interconnection of six-rings of tetrahedra with each six-ring connected to four neighbors through sharing common corners of the tetrahedra. The single layer contains 6-ring and 10-ring voids in a 1 : 1 ratio (Fig. 4(a)). The CuO_4 tetrahedron is highly distorted and may be considered as an intermediate between a regular tetrahedron and a planar square. The Cu–O bond lengths are in the range 1.920(2)–1.970 (2) Å. Four O–Cu–O bond angles are in the range 89.1(1)–98.1(8)° and two in the range 149.5(1)–153.9(1)°. The two independent Na sites both have a highly distorted octahedral coordination with Na–O bond lengths 2.298(2)–3.268(2) Å.

3.3.3. CuSH-4CsNa

The framework of *CuSH-4CsNa* contains double layers of SiO_4 tetrahedra interlinked by CuO_4 squares. The Cs ions are located in the voids inside the double layers while the Na ions and OH^- groups are located in the interlayer spaces (Fig. 5(a, b)). The silicate double layer is formed from two equivalent single layers (Fig. 5(c)). The single layer is formed
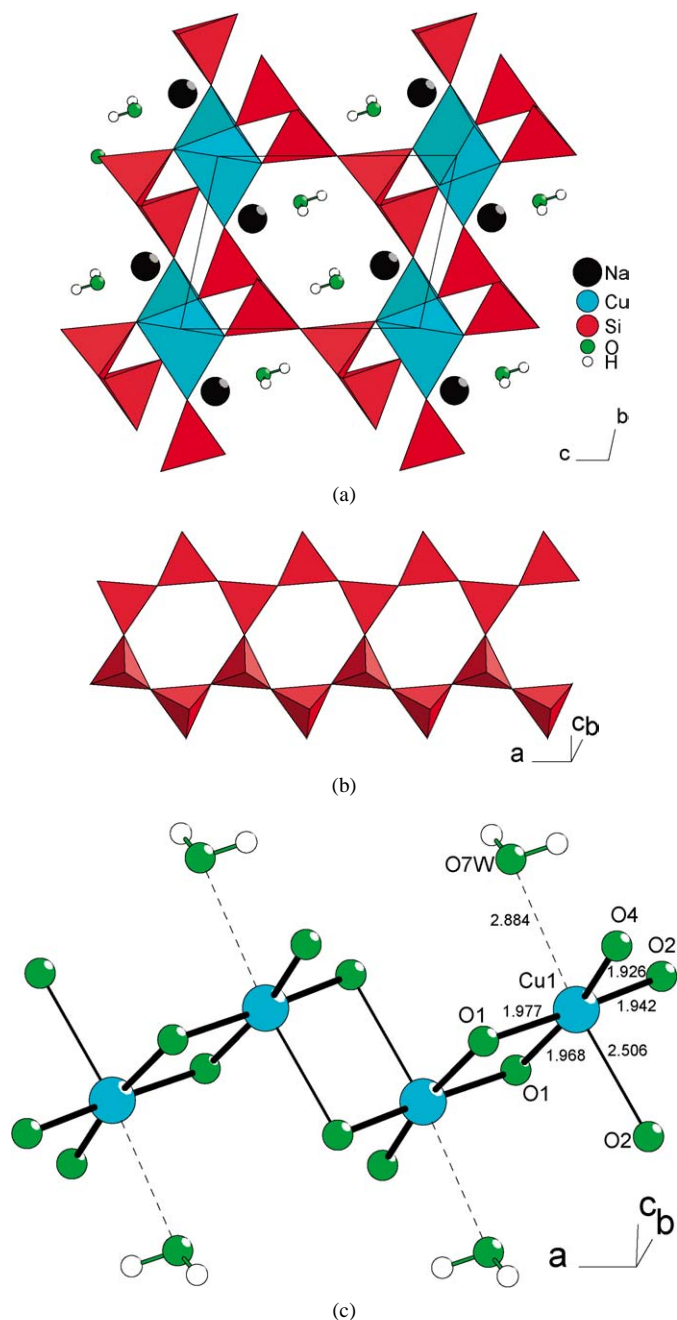
(a)

(b)

(c)

Fig. 3. The structure of CuSH-2Na. (a) Projection along [100]. (b) The double chain of silicate tetrahedra. (c) The chain of CuO$_5$ pyramids.

by connecting double chains of SiO$_4$ tetrahedra that are featured by 5-ring voids. Interconnection of the double chains gives rise to 8-ring voids in the single layer. The two single chains comprising the double chain are not the same. In one single chain three-connected SiO$_4$ tetrahedra dimers are alternatively linked by four-connected tetrahedron monomers while in the other single chain all the tetrahedra are three-connected and the corresponding dimers are linked by a tetrahedron with a terminal Si–OH group. The terminal corners of the dimers are shared with the interlayer CuO$_4$ squares that have Cu–O bond lengths 1.917(3)–1.942(3) Å. The Cs ion inside the silicate double layer is bonded to 10 oxygen atoms with Cs–O bond lengths

(a)

(b)

(c)
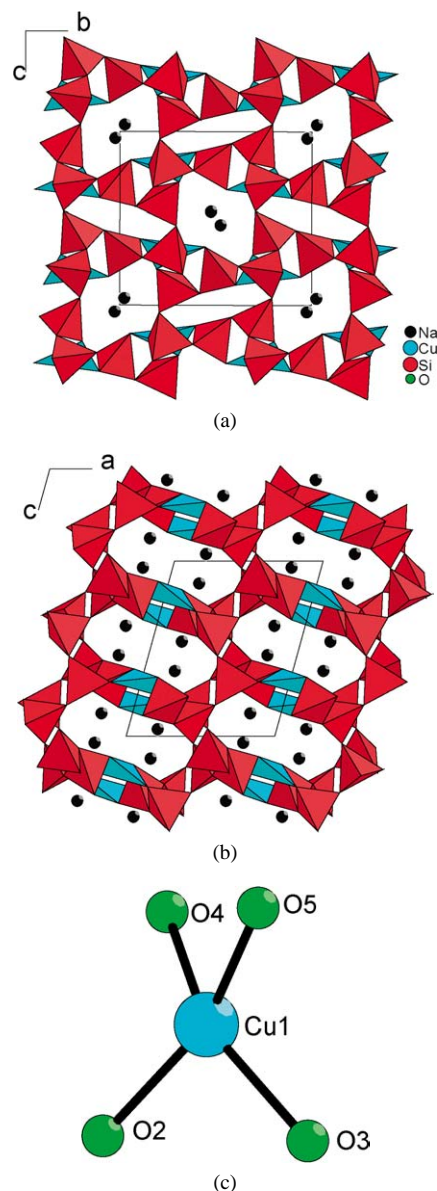
Fig. 4. The structure of CuSH-3Na (a) a view along [100]; (b) a view along [010]; (c) the distorted CuO$_4$ tetrahedron, O2–Cu1–O5: 153.1°, O3–Cu1–O4: 149.5°.

3.097(3)–3.650(3) Å. The two different Na sites are both co-ordinated to six oxygen atoms including oxygen atoms of a Si–OH group and a interstitial OH$^-$ ion with Na–O distances in the range 2.366(4)–2.654(4) Å. Relatively strong hydrogen bonds occur between the Si–OH groups and the interstitial OH$^-$ groups with an O···O distance of 2.675(6) Å.

3.3.4. CuSH-6Na

The structure of *CuSH-6Na* has a 1D system of 10-ring channels outlined by cross-linking single layers of SiO$_4$ tetrahedra through CuO$_5$ tetragonal pyramids (Fig. 6(a)). The silicate single layer is formed by bridging the double chains found in *CuSH-2Na* with two-connected SiO$_4$ tetrahedra (Fig. 6(b)). The CuO$_5$ tetragonal pyramids are interconnected into infinite edge-sharing chains closely similar to those of *CuSH-2Na* (Fig. 6(c)). The 10-ring channels are filled by Na ions and water mole-
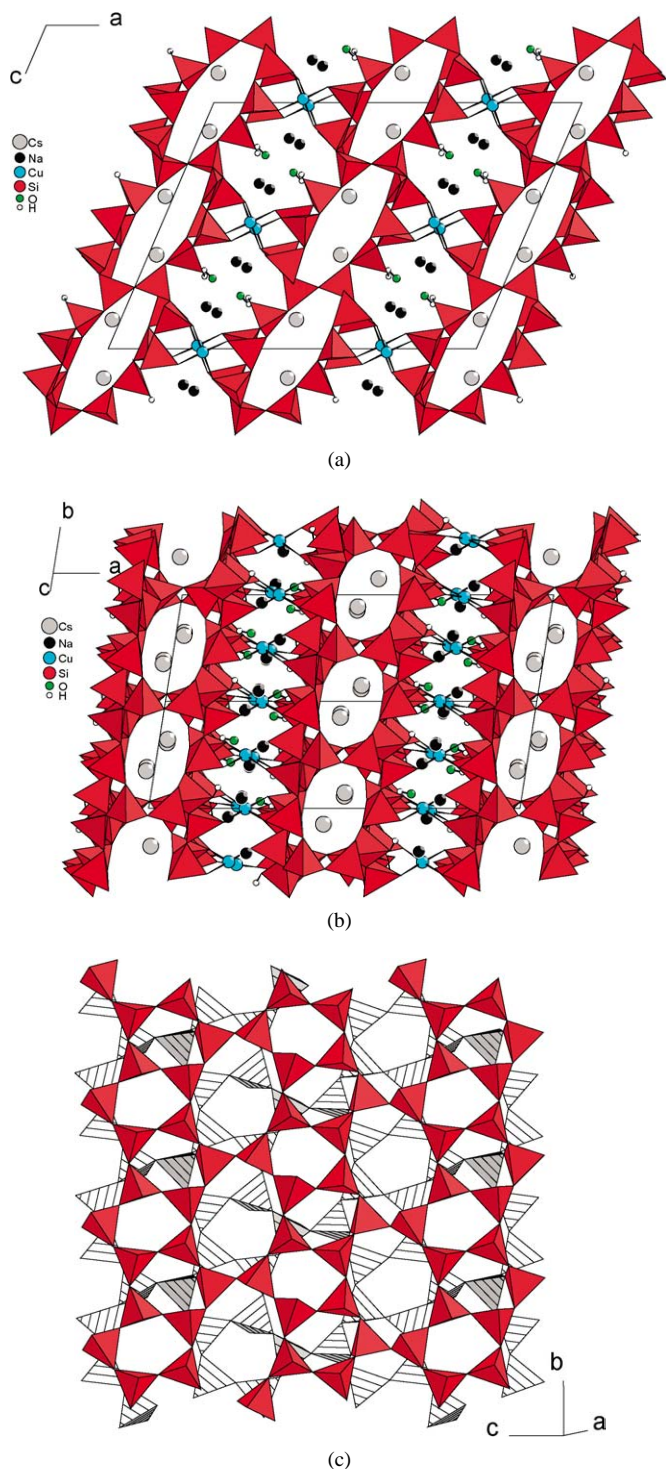
(a)

(b)

(c)

Fig. 5. The structure of CuSH-4CsNa. (a) Projection along [010]. (b) Projection along [011]. (c) The double layer of silicate tetrahedra, one single layer is marked by striping.

cules. The Na ion has a well defined octahedral coordination with Na–O distances 2.250(2)–2.542(2) Å. One of the two water molecule sites is split into two positions with an Ow···Ow separation of 1.858(6) Å. Well defined hydrogen bonds occur between the water molecules and the framework oxygen atoms with O···O distances 2.879(5)–2.965(3) Å which are weaker than the corresponding hydrogen bonds in *CuSH-2Na*.

(a)

(b)
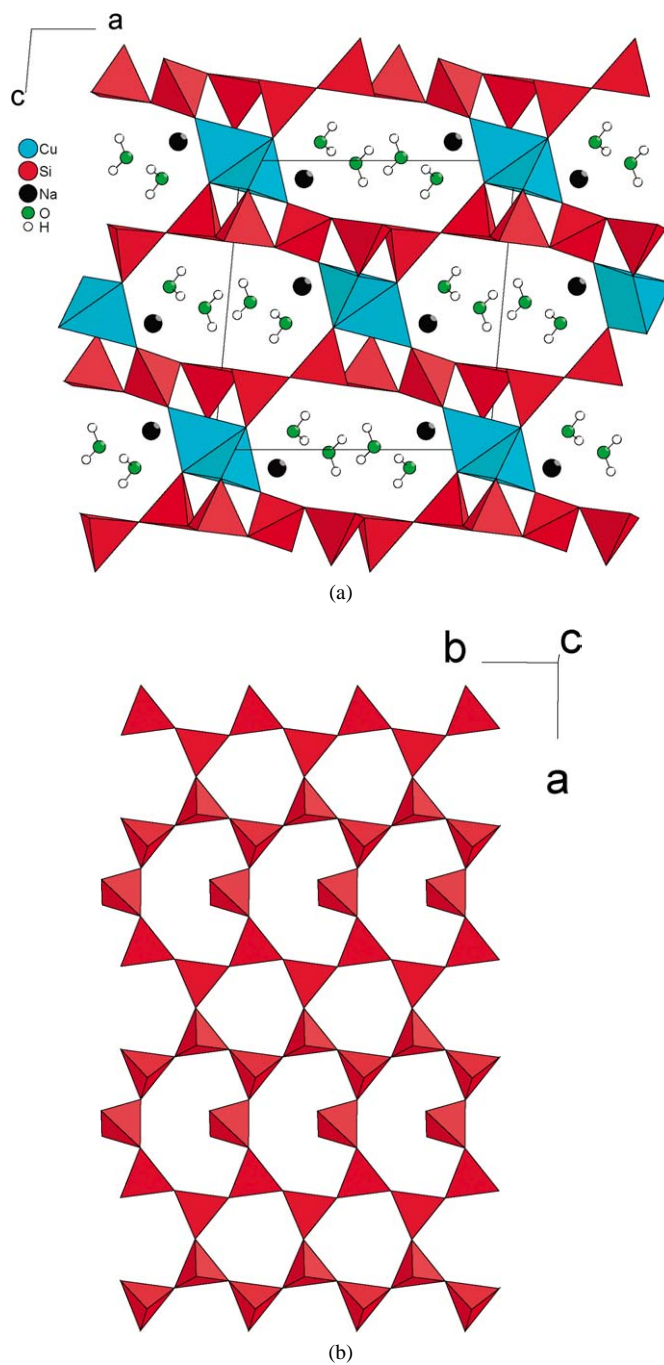
Fig. 6. The structure of CuSH-6Na. (a) Projection along [010]. (b) The single layer of silicate tetrahedra. (c) The chain of CuO$_5$ pyramids.

3.4. Structural comparison

3.4.1. CuSH-2Na, CuSH-6Na and related structures

The framework structure of *CuSH-6Na* may be considered as a simple expanded version of *CuSH-2Na* because the former can be derived from the latter by insertion of a column of separated SiO$_4$ tetrahedra between the double chains of *CuSH-2Na* and linking the double chains into the single layer of *CuSH-6Na* (Figs. 3, 6). The expansion substantially enhances the porosity of the framework and increases the aperture of the channels. While double chains similar to those present in
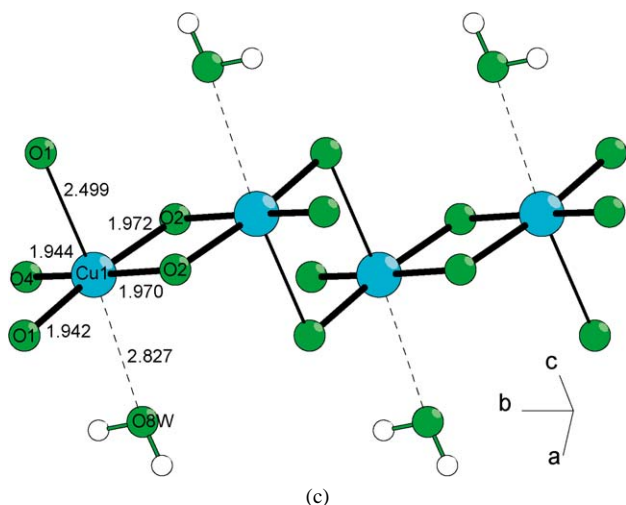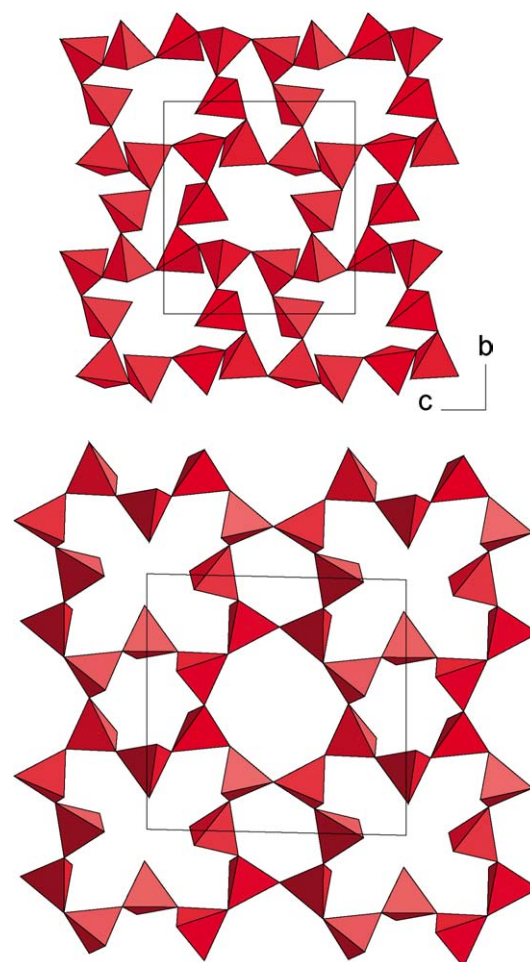
Fig. 6. Continued.

CuSH-2Na are found in a number of know silicates such as $Na_2H(NbO)Si_4O_{11}\cdot1.25H_2O$ [24] and the minerals of the amphibole group [11], the layer of *CuSH-6Na* is a novel type. It belongs to a rare group of single layers containing both three-connected and two-connected SiO_4 tetrahedra. In the minerals latiumite [25] and tuscanite [26], there are double layers of $(Al,Si)O_4$ tetrahedra which are formed from single layers closely similar to those in *CuSH-6Na*. The interesting relationship between the frameworks of *CuSH-2Na* and *CuSH-6Na* points to a promising way of building porous structures starting from other related multiple chain silicates.

3.4.2. CuSH-3Na and related structures

The silicate layer of *CuSH-3Na* also belongs to the rare group of single layers with both three-connected and two-connected SiO_4 tetrahedra. A similar silicate layer is found in the known compound $K_8Yb_3(Si_6O_{16})_2(OH)$ [27], which is formed by interconnection of 6-rings of SiO_4 tetrahedra in a similar way as in *CuSH-3Na* and also has both three-connected and two connected tetrahedra (Fig. 7). Judging from the position of the two-connected tetrahedra, the 6-rings in the layer of *CuSH-3Na* have roughly the same orientation while the 6-rings in $K_8Yb_3(Si_6O_{16})_2(OH)$ are perpendicular to each other. This orientation difference leads to 12-ring and 8-ring voids in the latter in contrast to the 10-ring voids in the former.

3.4.3. CuSH-4CsNa and related structures

There is a close similarity between the structures of *CuSH-4CsNa* and *CuSH-1A* [18]. Both structures are based on silicate double layers cross-linked by Cu–O bonds with interlayer Na ions and OH^- groups or water molecules. The silicate double layers of the two structures are substantially different, however, they have similar chains of 5-rings interconnected by four-connected tetrahedra and both can be constructed from the secondary-building-unit designated as "5-1" (a 5-ring with a branching tetrahedron) in the zeolite literature [2] (Fig. 8). Other related copper silicates with double layers include the mineral ajoite [13] and the synthetic compounds $A_2Cu_2Si_8O_{19}$ ($A =$ Rb, Cs) [28,29]. The double layers in these compounds are dominated by 6-rings of SiO_4 tetrahedra. Silicate single layers closely similar to that comprising the double layer of *CuSH-4CsNa* are found in the minerals nekoite $Ca_3Si_6O_{15}\cdot7H_2O$ [30], okenite $Ca_5Si_9O_{23}\cdot9H_2O$ [31] and zeravshanite $Cs_4Na_2Zr_3Si_{18}O_{45}\cdot2H_2O$ [32].

Fig. 7. Comparison of the single layers of CSH-3Na (top) and $K_8Yb_3(Si_6O_{16})_2(OH)$ [25] (bottom).

4. Conclusions

A series of novel open-framework copper silicate compounds have been synthesized in single crystal form under mild hydrothermal conditions. Structural studies reveal remarkable diversity both in the condensation of the silicate tetrahedra and in the copper oxygen coordination polyhedra connected to the silicate anions. Compared to the wide 12-ring channels of the CuSH-1A materials reported previously, the channels in the compounds reported here are narrower with 8-ring or 10-ring sections.

The low temperature hydrothermal reaction conditions led to several structure features in the CuSH-*n* series that are not observed in the copper silicates synthesized at high temperatures. These include frameworks containing terminal $SiO_3(OH)$ units and water molecules, and salt inclusion in the channel systems
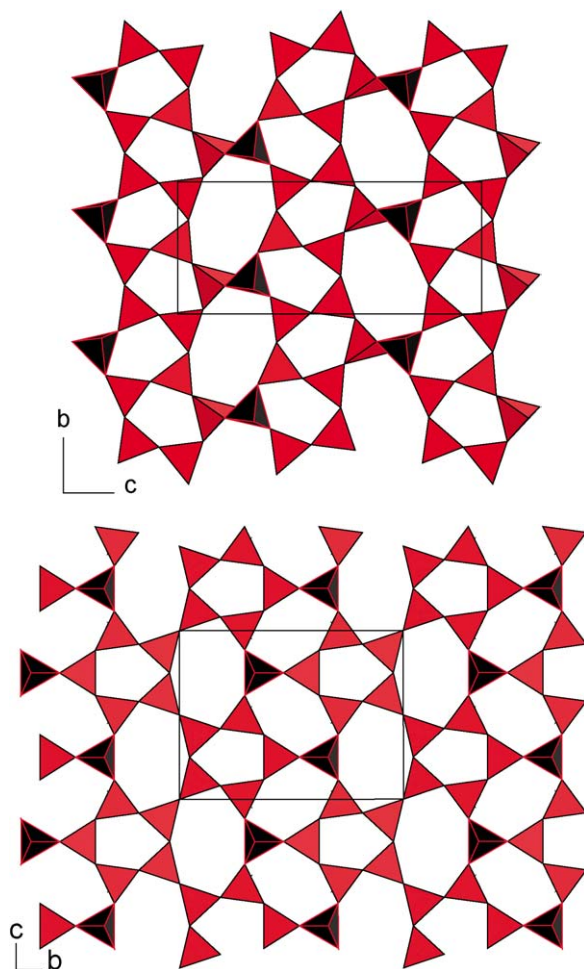
Fig. 8. Comparison of the silicate single layers of CuSH-4CsNa (top) and CuSH-1Na (bottom). The four-connected tetrahedra linked to the other single layer of the double layers are marked by black color.

as shown by CuSH-1 and CuSH-4. In contrast to the VSH-n series of vanadium silicates where the silicate anions are dominated by simple single layers with three-connected tetrahedra, the copper silicates show more structural complexity. In fact, the simple single layers comprising only three-connected SiO_4 tetrahedra have not been observed in the copper silicates. Instead, they tend to be interrupted by two-connected tetrahedra or to segregate into double layers to produce tubular structures. The linking copper–oxygen polyhedra can vary from distorted tetrahedra as in CuSH-3 to squares, square pyramids or elongated octahedra as in ajoite where the CuO_6 octahedra condense into brucite layers. Further structural diversity can be achieved by introducing a second transition metal element into the frameworks as shown in the system of copper titanosilicates [23].

References

[1] M.E. Davis, Nature 417 (2002) 813.
[2] H.V. Bekkum, E.M. Flanigen, P.A. Jacobs, J.C. Jansen, Introduction to Zeolite Science and Practice, Elsevier, Amsterdam, 2001.
[3] Z. Gabelica, S. Valance, Res. Chem. Intermed. 24 (1998) 227.
[4] J. Rocha, M.W. Anderson, Eur. J. Inorg. Chem. (2000) 801.
[5] S.M. Kuznicki (Engelhard Corp.), U.S. Patent 4,853,202, 1989; U.S. Patent 4,938,939, 1990.
[6] J. Rocha, P. Brandao, Z. Lin, M.W. Anderson, V. Alfredsson, O. Terasaki, Angew. Chem., Int. Ed. Engl. 36 (1997) 100.
[7] X. Wang, L. Liu, A.J. Jacobson, Angew. Chem. Int. Ed. 40 (2001) 2174.
[8] X. Wang, L. Liu, A.J. Jacobson, J. Am. Chem. Soc. 124 (2002) 7812.
[9] J. Huang, X. Wang, L. Liu, A.J. Jacobson, Solid State Sci. 4 (2002) 1193.
[10] C.-Y. Li, C.-Y. Hsieh, H.-M. Lin, H.-M. Kao, K.-H. Lii, Inorg. Chem. 41 (2002) 4206.
[11] F. Liebau, Structural Chemistry of Silicates, Springer-Verlag, Berlin, 1985.
[12] A. Pabst, Acta Cryst. 12 (1959) 733.
[13] J.J. Pluth, J.V. Smith, Proc. Nat. Acad. Sci. USA 99 (2002) 11002.
[14] B.J. Hathaway, Structure and Bonding 57 (1984) 55.
[15] P.C. Burns, F.C. Hawthorne, Canad. Mineral. 34 (1996) 1089.
[16] X. Wang, L. Liu, J. Huang, A.J. Jacobson, Acta Cryst. A 58 (Suppl.) (2002) C185.
[17] A.J. Jacobson, X. Wang, L. Liu, J. Huang, MRS Fall Meeting, 2002, Boston;
A.J. Jacobson, X. Wang, L. Liu, J. Huang, Mater. Res. Soc. Symp. Proc. 755 (2003) 63.
[18] X. Wang, L. Liu, A.J. Jacobson, Angew. Chem. Int. Ed. 42 (2003) 2044.
[19] P. Brandao, F.A.A. Paz, J. Rocha, Chem. Commun. (2005) 171.
[20] SAINT, Program for Data Extraction and Reduction, Siemens Analytical X-Ray Instruments Inc., Madison, USA, 1996.
[21] G.M. Sheldrick, SADABS, Program for Siemens Area Detector Absorption Corrections, University of Gottingen, Germany, 1997.
[22] G.M. Sheldrick, SHELXTL, Program for Refinement of Crystal Structures, Siemens Analytical X-Ray Instruments Inc., Madison, USA, 1994.
[23] X. Wang, L. Liu, L. Wang, A.J. Jacobson, Mater. Res. Soc. Symp. Proc. 848 (2005) FF3.2.
[24] M.A. Salvado, P. Pertierra, S. Garcia-Granda, S.A. Khainakov, J.R. Garcia, A.I. Borturn, A. Clearfield, Inorg. Chem. 40 (2001) 4368.
[25] E. Cannillo, A. Dal Negro, G. Rossi, Amer. Mineral. 58 (1973) 466.
[26] M. Mellini, S. Merlino, G. Rossi, Amer. Mineral. 62 (1977) 1114.
[27] D.Yu. Pushcharovskii, A.M. Dago, E.A. Pobedimskaya, N.V. Belov, Dokl. Akad. Nauk SSSR 258 (1981) 1111.
[28] A. Heinrich, V. Gramlich, Naturwissenschaften 69 (1982) 142.
[29] I. Watanabe, A. Kawahara, Acta Cryst. C 49 (1993) 854.
[30] A. Alberti, E. Galli, Amer. Mineral. 65 (1980) 1270.
[31] S. Merlino, Amer. Mineral. 68 (1983) 614.
[32] Y.A. Uvarova, E. Sokolova, F.C. Howthorne, L.A. Pautov, A.A. Agakhnov, Canad. Mineral. 42 (2004) 125.